ELSEVIER

Environmental Pollution 116 (2002) S255–S268

ENVIRONMENTAL POLLUTION

www.elsevier.com/locate/envpol

Use of pyrolysis molecular beam mass spectrometry (py-MBMS) to characterize forest soil carbon: method and preliminary results

K.A. Magrini[a,*], R.J. Evans[a], C.M. Hoover[b], C.C. Elam[a], M.F. Davis[a]

[a]*National Renewable Energy Laboratory, 1617 Cole Blvd., Golden, CO 80401, USA*

[b]*USDA Forest Service, Northeastern Research Station, PO Box 267, Irvine, PA 16329, USA*

"Capsule": *Changes in soil organic matter chemical composition were successfully characterized using applied pyrolysis molecular beam mass spectrometry on whole soil samples*

Abstract

The components of soil organic matter (SOM) and their degradation dynamics in forest soils are difficult to study and thus poorly understood, due to time-consuming sample collection, preparation, and difficulty of analyzing and identifying major components. As a result, changes in soil organic matter chemical composition as a function of age, forest type, or disturbance have not been examined. We applied pyrolysis molecular beam mass spectrometry (py-MBMS), which provides rapid characterization of SOM of whole soil samples, to the Tionesta soil samples described by Hoover, C.M., Magrini, K.A., Evans, R.J., 2002. Soil carbon content and character in an old growth forest in northwestern Pennsylvania: a case study introducing molecular beam mass spectrometry (PY-MBMS). Environmental Pollution 116 (Supp.1), S269–S278. Our goals in this work were to: (1) develop and demonstrate an advanced, rapid analytical method for characterizing SOM components in whole soils, and (2) provide data-based models to predict soil carbon content and residence time from py-MBMS analysis. Using py-MBMS and pattern recognition techniques we were able to statistically distinguish among four Tionesta sites and show an increase in pyrolysis products of more highly decomposed plant materials at increasing sample depth. For example, all four sites showed increasing amounts of older carbon (phenolic and aromatic species) at deeper depths and higher amounts of more recent carbon (carbohydrates and lignin products) at shallower depths. These results indicate that this type of analysis could be used to rapidly characterize SOM for the purpose of developing a model, which could be used in monitoring the effect of forest management practices on carbon uptake and storage.

Keywords: Pyrolysis mass spectroscopy; Soil organic carbon; Forest soils; Rapid soil analysis; Disturbance

1. Introduction

Forest soil carbon is one of the most poorly understood global carbon pools. This is partly due to the difficulty and expense of current techniques available to measure soil carbon components and soil carbon changes and partly due to spatial variability and the difficulty of obtaining representative samples. As a result, the uncertainty in soil carbon knowledge is so great that opposition exists to giving credit for forest soil carbon sequestration in international greenhouse gas negotiations. The perception is that it will be difficult, if not impossible, to verify claims that carbon is actually being absorbed and retained in soils, a problem that is compounded by the fact that the dynamics and chemistry of soil organic matter (SOM) are not well understood. The work described here begins to address the need to develop and demonstrate analytical techniques that can rapidly provide information on soil carbon concentration and chemistry, information that is crucial to verifying carbon uptake and storage in the largest terrestrial pool–soil (Rosenberg et al., 1998).

A primary component of soil organic matter comes from the decomposition of biomass-derived materials. The resulting humic substances vary greatly in their decomposition rates, and when accurately measured, provide a foundation for estimating the uptake of carbon in soils. Separating and measuring these components with classical techniques is both difficult and complex. Most soil analyses require mechanical preparation, extraction and one or more chemical analyses; processes which are time consuming and labor intensive. Such methods include wet chemical digestion, extraction, and instrumental analyses for mineral, metal, and organic species; thermoanalytical techniques for moisture, nitrogen, carbon, and sulfur content (Schepers et al., 1989; Beyer et al., 1998), and physical characterization of surface area, particle fractions, and adsorbents. Wet chemical and instrumental methods have been developed for

* Corresponding author. Fax: +1-303-384-6363.
E-mail address: kim_magrini@nrel.gov (K.A. Magrini).

0269-7491/01/$ - see front matter
PII: S0269-7491(01)00257-3

separating and quantifying fulvic, humic, and lignin soil fractions (Ogner and Schnitzer, 1971; Tao et al., 1997). The $^{14}C/^{12}C$ ratio can be used to estimate organic content age (Scharpenseel, 1975). Taken together, these analytical techniques can comprehensively describe soil samples, though the time required is significant and not easily done on large numbers of samples. Moreover, some analyses may not be representative of the original material due to the harsh chemical separations used.

Recent applications of spectroscopic methods to soils have begun to address the need for comprehensive SOM analysis. Specific techniques include near infrared (NIR) spectroscopy, pyrolysis-gas chromatography mass spectrometry (py-GC/MS), and pyrolysis field ionization mass spectrometry (py-FIMS). NIR is a fast technique that can determine total carbon and moisture but it cannot speciate soil carbon compounds, which are useful for verifying soil carbon uptake (Salgo et al., 1998; Reeves et al., 1999). Py-GC/MS has been used to investigate a wide range of plant materials and humic substances, though few investigations of whole soils have been reported. Recent work has cataloged individual pyrolysis mass spectra obtained from py-GC/MS of the protein, carbohydrate, and humic fractions of soil organic carbon (Stuczynski et al., 1997). Tresar-Cepada et al. (1994) used py-GC/MS to characterize extracted humic and fulvic species from 4- and 7-year-old lignite mine soils and found that with soil age there is a marked decrease in mineralizable substances (carbohydrates and lignins) and an increased concentration of aromatic substances (benzene and toluene). This shows that the degree of humification of organic matter increases progressively.

Analytical pyrolysis (py) has been widely applied to structural studies of synthetic and biologic macromolecules. The transfer of thermal energy to the polymeric network or macromolecule causes physical cleavage of the chemical bonds and yields pyrolysis products that are characteristic of the original structures. Schulten has extensively developed py-FIMS for the study of whole soils and soil fractions (Schulten, 1996; Schulten and Leinweber, 1999). This method has been applied to structural investigations of plant and litter components and organic matter in varied soils. The FIMS method is not suited for rapid analyses as each sample must be inserted into the ionization region of the mass spectrometer and individually analyzed. In addition, the microgram quantities typically used may not allow whole (unprepared) soil samples to be analyzed without significant sample preparation.

An early py-FIMS application assessed forest management practices by analyzing differences in the dissolved organic matter in soil leachates from under pine and oak forests (Hempfling and Schulten, 1990). Py-FIMS has been used to study short-term (seasonal) SOM dynamics in whole soil samples with spectra clearly showing qualitative changes in the SOM composition during the growing season. Variations in the abundance of signals for carbohydrates and nitrogen-containing compounds occurred during periods as short as a few weeks and were more pronounced in fertilized soils (Leinweber et al., 1993). This work indicates that mass spectroscopic techniques can be applied to studying carbon uptake in soils actively managed for carbon storage in the time frame of months to years.

Very recent work has combined wet chemistry, ^{13}C NMR spectroscopy and py-FIMS with multivariate statistical analysis to characterize whole soils from nine different podzol B-horizons. Chemometric analysis of the pooled data showed that only py-FIMS distinguished the B-horizons according to SOM composition (Wilcken et al., 1997). Py-FIMS can be used with other analytical techniques to monitor molecular chemical changes of SOM composition and stability in soil chronosequences (Leinweber et al., 1996). Other work has compared SOM in co-located forest and agricultural soils. Gregorich et al. (1996) used ^{13}C NMR and py-FIMS to characterize plant tissue, isolated soil fractions, and whole surface soils and subsurface soils from a forest system and a maize system. Both techniques indicated that the plant material entering the soil in forest and maize-cropped soil was chemically different. The work presented here builds on the results of soil analysis with py-FIMS by coupling the pyrolysis technique with molecular beam mass spectrometry and multivariate statistical analysis to rapidly and accurately characterize forest soil carbon content, species, and age.

2. Materials and methods

Mass spectrometry is a technique for materials analysis that relies on conversion of a sample into a gaseous ionic form, followed by separation of the ions according to their mass-to-charge ratio (m/z). The information produced from this technique is presented as a mass spectrum, which shows the relative amounts of different ions formed in the spectrometer under specific conditions.

A typical mass spectrometer consists of an ion source, where the sample is introduced as a gas or converted into the gas-phase by heating and then ionized. In the next section, the mass analyzer, the ions produced in the ion source are sorted into beams of ions of the same mass-to-charge ratio. In the detection system, the mass sorted ions are electronically detected.

The most useful applications of mass spectrometry are molecular weight determinations of volatile compounds and structural analysis from the distribution of peak heights at different mass-to-charge ratios. Quantitative analysis of solids and liquids can also be performed with various methods for ionizing the material to be analyzed.

We have developed the pyrolysis-molecular beam mass spectrometer (py-MBMS) technique for analyzing

a wide range of large and complex biomolecules that include lignins, cellulosic materials, plastics, and polymers. This work applies the technique to whole soils. The method we used consists of rapidly heating soil samples (0.1 g) in an inert, helium atmosphere at 500 °C. This process takes place at ambient pressure in a quartz reactor, which is connected to the inlet of the MBMS (Fig. 1). The generated pyrolysis products are sampled directly in real time by expanding through a sampling orifice with subsequent formation of the molecular beam, which provides rapid sample quenching and inhibits sample condensation. These sampling characteristics are important for analyzing complex molecules because they retain the chemical structure of large fragments of the original chemical species. The details of this type of sampling are discussed in several papers (Milne and Soltys, 1983; Evans et al., 1986; Evans and Milne, 1987) The mass spectrometer provides universal detection of all sampled products and the molecular beam sampling ensures that representative products from the original molecules are detected. For this work, we used a mass range of 15–350 amu. The molecular beam method of sample generation is rapid (1–5 min) and provides sample throughputs of 100–200 samples per day depending on analytical conditions.

To demonstrate the feasibility of this technique for soil carbon analysis, we analyzed whole soil samples, taken from four sites at three depths, from the Tionesta Scenic and Research Natural Areas of the Allegheny plateau of northwestern Pennsylvania. These sites, where major stand replacing wind events of the original 600-year-old virgin beech hemlock stands have occurred at approximately 100-year intervals, were chosen to determine if py-MBMS could distinguish carbon content and speciation for both site (varied vegetation) and sample depth. The samples were also analyzed with combustion MBMS for total carbon content. Combustion results are presented in Hoover et al. (2002).

The sampling protocol is only summarized here. In each of the 1808, 1872, and 1985 blowdown areas, and in an intact virgin beech-hemlock stand, a 0.2 ha plot was established. In each study plot, 16 soil cores were collected on a systematic grid; forest floor material was removed and only mineral soil was sampled. Cores were 5 cm in diameter, and were divided into 0–5, 5–15, and 15–30 cm depth increments. The 16 cores were composited in the field by depth increment to form four samples per depth increment per plot for analysis. Samples were dried and sieved through a 2-mm screen prior to sending to NREL for MBMS analysis.

Soil samples (~0.1 g) were weighed in quartz boats in triplicate and pyrolyzed in a reactor consisting of a quartz tube (2.5 cm inside diameter) with helium flowing through at 5 l/min (at STP). The reactor tube was oriented so that the sampling orifice of the MBMS was inside the end of the quartz reactor. We used a molecular beam system comprised of an ExtrelTM Model TQMS C50 mass spectrometer for both pyrolysis and combustion vapor analysis. The reactor was electrically heated and its temperature maintained at 500 °C. Total pyrolysis time was 5 min. The residence time of the pyrolysis vapors in the reactor pyrolysis zone was estimated to be ~75 ms. This residence time is short enough that secondary cracking reactions in the quartz reactor are minimal. Mass spectral data from 15–350 amu were acquired on a Teknivent Vector 2™ data acquisition system using 22 eV electron impact ionization. Data acquisition was continuous, through digitization of electron-multiplier signals from the arrival of positive ions and programmed storage in an IBM PC computer. Repetitive scans (typically one 300 amu scan/s) were recorded during the evolution of a pyrolysis wave from each soil sample. The stored spectra could be manipulated to give average spectra, subtracted spectra, or time evolution of different masses. Using this system, both light gases and heavy molecules are sampled simultaneously and in real time. The mass spectrum of

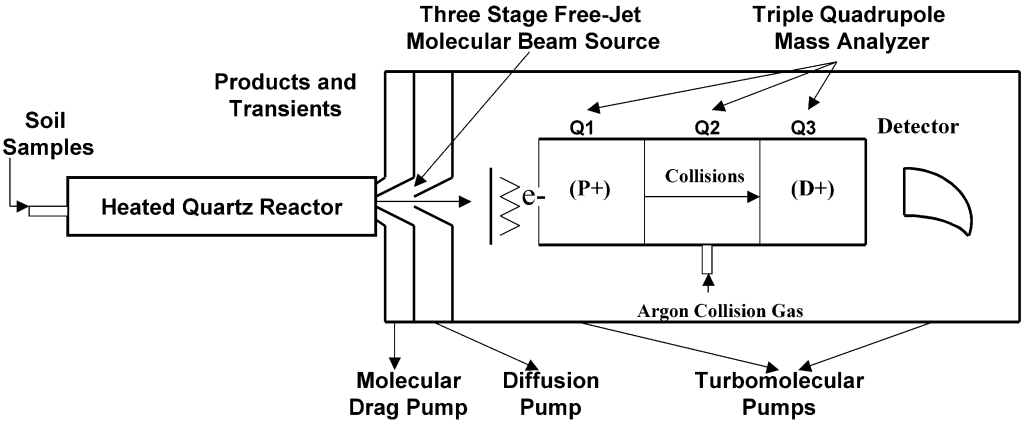

Fig. 1. Schematic representation of the molecular beam sampling mass spectrometer (py-MBMS) system. The soil samples were introduced into the heated quartz reactor for pyrolysis and combustion analysis.

the pyrolysis vapor provides a rapid, semiquantitative picture of the molecular fragments (Evans and Milne, 1987; Tuskan et al., 1999).

The resultant pyrolysis mass spectra are very complex. We used multivariate data analysis (pattern recognition) to handle this large data set and identify trends to discover the underlying chemical changes that may not be obvious by comparison of such complex mass spectra (Windig et al., 1987; Agblevor et al., 1994).

The first step in data processing was to average the 20–30 spectra that were accumulated while each sample pyrolyzes. The time-resolved information is not used for these analyses, although it will likely reveal additional information. The average spectra are then normalized to 100% total ion intensity, which corrects for differences in sample size and organic matter content of the samples. This means that the py-MBMS comparisons in this paper are based on the composition of the organic SOM.

The matrix of normalized data is then scaled such that each mass has an equal variance. This means that in factor analysis small masses are equally weighted as large ones. This is done by dividing each mass variable intensity by the standard deviation for that mass variable for all samples. The ISMA (Interactive Self-Modeling Multivariate Analysis) program was used for factor analysis (Windig et al.,1987). Factor analysis is performed on the correlation around the origin matrix in ISMA for the resolving of components from complex mixtures where standards and calibration references are not available. This is further discussed in Section 3.

Other statistical analyses were performed using an SPSS Base 10.0 statistical analysis program for the PC (SPSS, 1999). This included univariate, ANOVA, correlation, regression and discriminant analyses. Discriminant analysis is a method of classification where multivariate data on replicated samples is used to define models that optimally separate classes of samples. In this case, the factor scores that resulted from factor analysis were used as the multivariate data for discriminant analysis. The factor scores are ideally suited for discriminant analysis since they are orthogonal (uncorrelated) by definition. Each sample group is defined by a discriminant function which is a linear combination of the factor scores that maximizes the ratio of the between groups to within group variances. The results can then be tested to see how well it predicts the classes of the data set.

3. Results and discussion

A typical profile of soil pyrolysis product evolution is shown in Fig. 2 where eight samples were run in a period of 14 min. A measure of the total ion intensity (TII) is plotted and the total organic carbon values are indicated above each sample. The overall correlation coefficient between TII and total organic carbon is $r^2 = 0.9$ but for low amounts of carbon the correlation is less favorable since there is likely a higher amount of carbon that is converted to nonvolatile products. For the comparisons in this paper, the spectra were integrated for

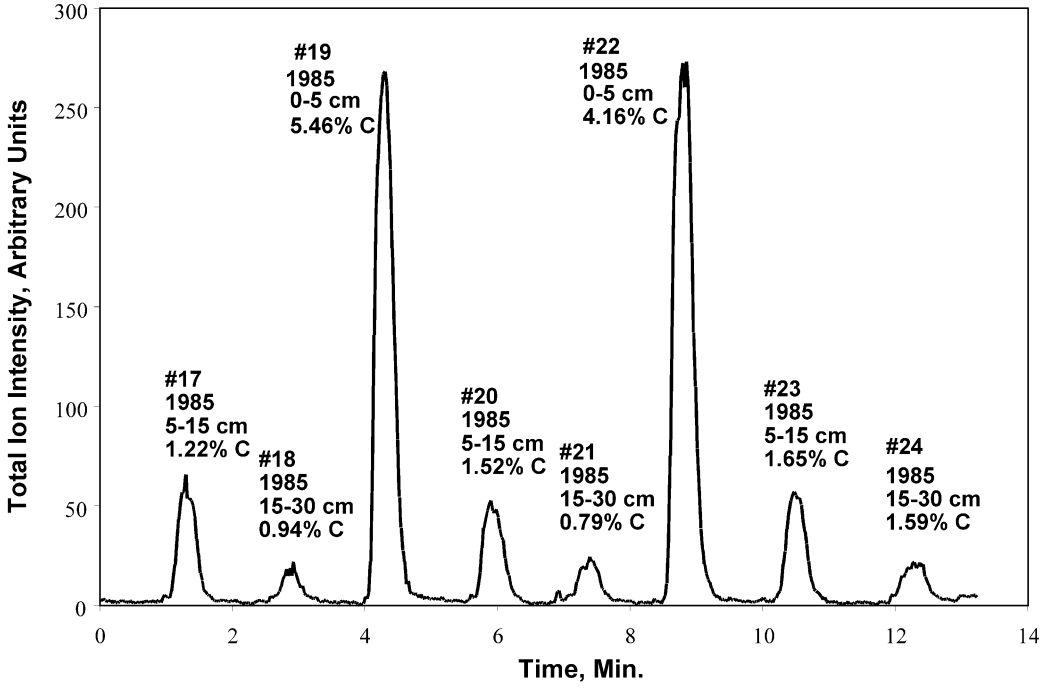

Fig. 2. A typical profile of soil pyrolysis product evolution for eight samples run in a period of 14 min. Total ion intensity, the sum of all ions for each mass spectrum, is plotted.

each sample and the distribution of masses presented as the % of TII. Each sample is treated equally in the subsequent analysis by using this normalized data regardless of its carbon content or relative TII. The samples shown in Fig. 2 were part of the 107 samples included in this work. The short timeframe shows the rapid nature of this analysis and the potential for screening large number of soil samples for characterizing organic carbon species.

Two examples of integrated spectra are shown in Fig. 3: (a) a 0–5 cm sample and (b) a 15–30 cm sample from the 1985-blowdown series. The 0–5 cm sample has a greater abundance of peaks attributable to recent biomass, such as carbohydrate-derived peaks (m/z 60, 73, 98, 126) and lignin-derived peaks (m/z 124, 138, 150). Major peaks at m/z 82 and 96 are sometimes due to more severe thermal degradation of carbohydrates, especially from the pentosans in the hemicellulose fraction of wood (Evans and Milne, 1987). The major peaks at m/z 110, 122 and 136 are derived similarly from the more severe thermal degradation of lignin (Evans and Milne, 1987). These changes can be achieved by treating the initial pyrolysis products to additional gas phase pyrolysis or by pretreating the solid at lower temperature before exposing it to high temperature. This suggests that the predominance of these mass peaks (m/z 82, 96, 110, 122, and 136) over the more typical primary pyrolysis products (m/z 60, 73, 98, 124, 126, 138, and

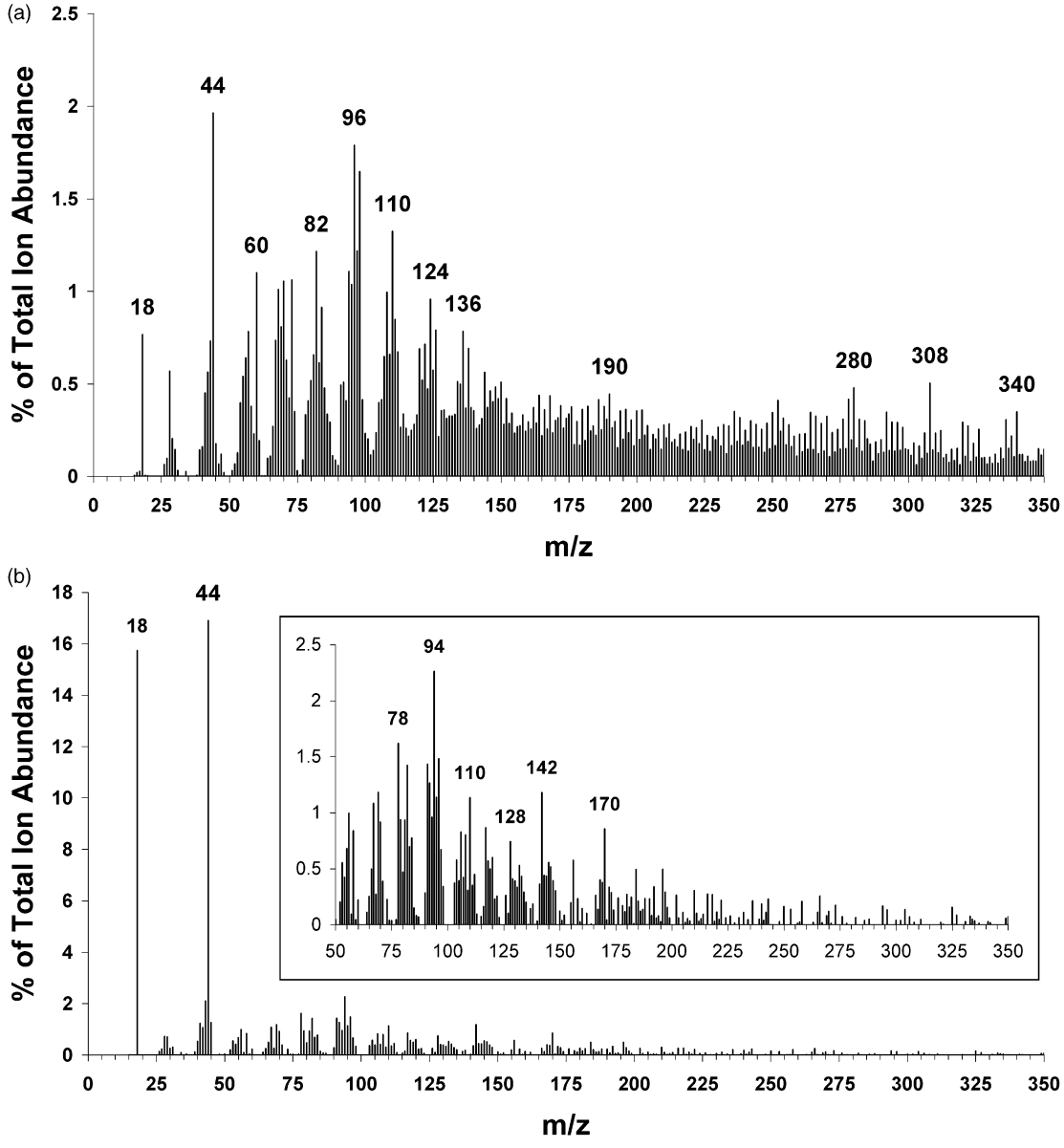

Fig. 3. Integrated spectra for (a) 0–5-cm and (b) 15–30-cm samples from the pyrolysis molecular beam mass spectrometry (py-MBMS) analysis of the 1985 blowdown series. The mass spectra that occurs over pyrolysis molecular beam mass spectrometry the pyrolysis wave for each sample are averaged. Higher mass ranges are shown in the inset of (b).

150) is an indication that the same type of dehydration, decarbonylation, and condensation reactions has altered the organic matter in the soil, probably by microbial processes over time. The spectra from these soils are more complicated than those observed for wood, and many of the major peaks in the higher mass range in Fig. 3a are not attributable to known biopolymer pyrolysis, such as m/z 280, 308, and 340. They are not typical of distributions observed from lignin or wood, nor are they similar to other major compound classes that may be associated with unaltered soil organic matter constituents, such as lipid materials.

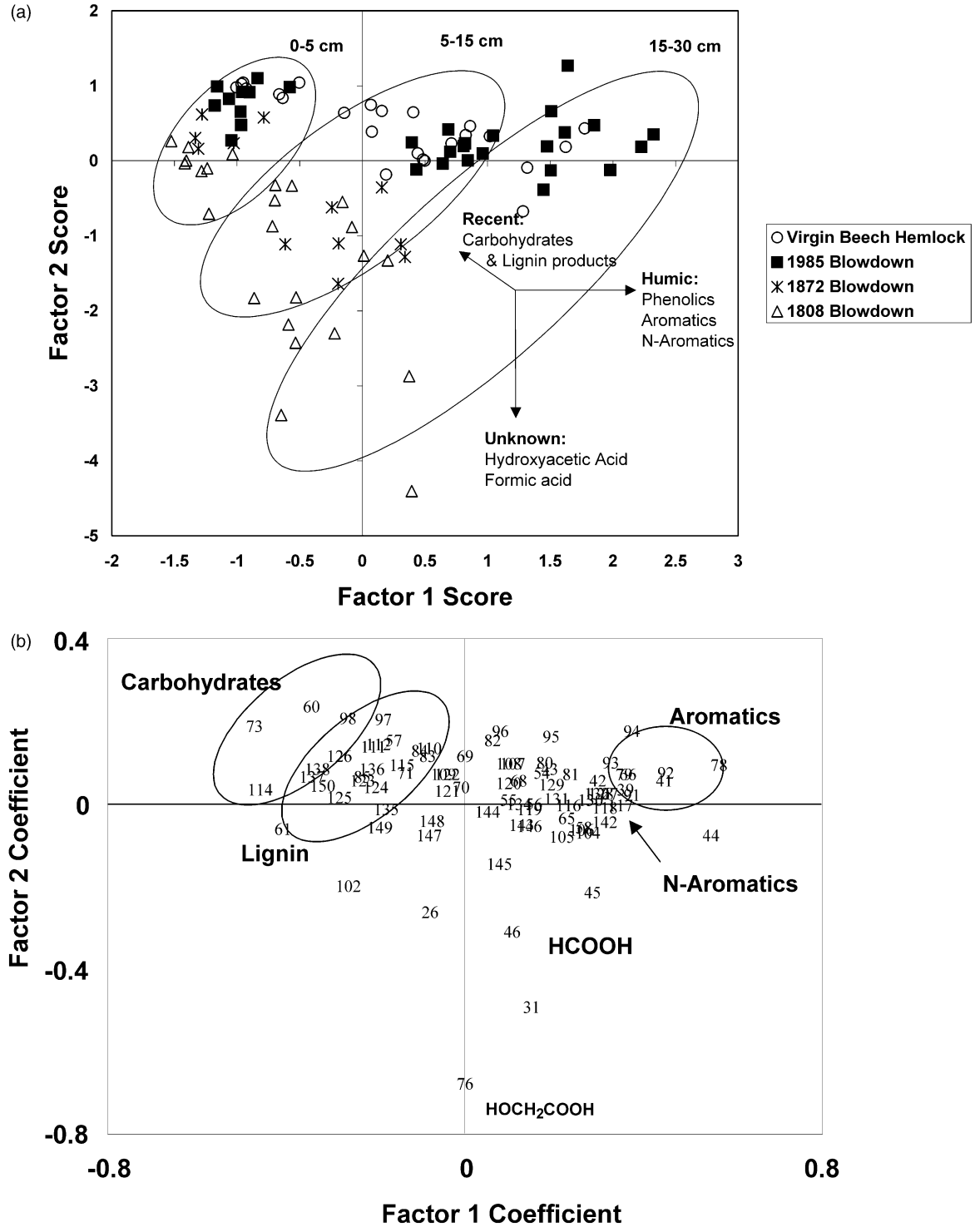

Fig. 4. Results of factor analysis: (a) the factor score plot for the 107 samples in the database. Factors one and two explain 35 and 11% of the variance, respectively. (b) The mass-variable coefficients (loadings) for the two factors plotted in (a).

In the 15–30 cm sample shown in Fig. 3b the pyrolysis products are dominated by water (m/z 18) and CO_2 (m/z 44). The higher mass range is shown expanded in the insert and we see the predominance of monoaromatics (benzene, 78; toluene, 92; and xylene, 106), phenolics (phenol, 94; cresol, 108; catechol, 110); and polyaromatics (naphthalene, 128; and methylnaphthalenes, 142, 156, 170). Nitrogen-containing aromatics (e.g. indole, 117) are also present.

For such complicated data sets, simple data analysis by the comparison of two spectra is of limited use. Multivariate analysis, proven to be an important tool for pattern recognition in pyrolysis mass spectrometry, shows both the similarities and differences between samples, and additionally shows correlated behavior among the mass variables (Evans and Milne, 1987). We used this approach, first to evaluate the structure of the data set and determine the extent to which the patterns associated with site and depth are observable, and then to calculate the subspectra responsible for differences that could be interpreted chemically. Factor analysis was performed using the average mass spectra for each sample. Fig. 4a shows the factor score plot for the 107 samples in the database. The factor scores are weighted combinations of the relative abundances, in which each mass is weighted by its correlation coefficient with the factors. The factors are orthogonal to each other and calculated to explain the maximum amount of variance in the data set. In this data set the first four factors explain 35, 11, 6.5 and 3.7% of the variance, respectively. The score plots are an efficient way to show the variance in the data set and the differentiation of classes of samples based on the py-MBMS results. Fig. 4a shows that the first two factors can differentiate the samples based on site and depth. The three ellipses show the groupings for soil depths and the symbols show the different sites (i.e. virgin forest and wind events in 1985, 1872, and 1808). Clearly, the differentiation of site can be shown even in the top horizon.

To test the extent to which the replicated samples can be discriminated by this characterization technique, the factor scores were subjected to discriminant analysis. Discriminant analysis is used to determine the ability of the characterization variables and the factor scores to predict the classification of samples. Twelve cases were tested: three depths at four different sites. The results are shown in Table 1. The misclassifications were either at the same depth from the closest age site or as the adjacent profile. These results are dependent on the number of factors used. However if only three factors are used instead of six, then the correct percentage only drops from 76 to 64% and the misclassifications follow the same trend as shown in Table 1. These results are encouraging in that a model of organic matter, age, and composition can be constructed based on py-MBMS once the underlying chemistry has been understood. This, however, is beyond the scope of this initial study. For further discussion of the soil science implication of this work, see the accompanying paper by Hoover et al. (2002).

We can show the underlying chemistry that drives the clustering of samples by looking at the masses that are most important in defining factors one and two. Fig. 4b shows the loadings for the two factors that are plotted in Fig. 4a. This plot shows the underlying chemistry that causes the separation of classes of samples. Fig 4a indicates that the major source of variance in factor one is due to sample depth. Fig 4b provides a chemical explanation by the presence of higher amounts of aromatics and nitrogen-containing aromatics in the pyrolysis products for the 15–30 cm depth samples, and higher amounts of primary pyrolysis products from

Table 1
Classification results based on discriminant analysis of the top six factor scores for replicated pyrolis molecular beam mass spectrometry analyses and multiple samples at each site for three depth profiles at the four sites[a]

Site	Depth	Class	Predicted group membership											
			1	2	3	4	5	6	7	8	9	10	11	12
Virgin	0–5	1	*38*	12	0.0	50	0.0	0.0	0.0	0.0	0.0	0.0	0.0	0.0
	5–15	2	0.0	*75*	0.0	0.0	25	0.0	0.0	0.0	0.0	0.0	0.0	0.0
	15–30	3	0.0	13	*50*	0.0	25	12	0.0	0.0	0.0	0.0	0.0	0.0
1985	0–5	4	10	0.0	0.0	*90*	0.0	0.0	0.0	0.0	0.0	0.0	0.0	0.0
	5–15	5	0.0	10	10	0.0	*70*	10	0.0	0.0	0.0	0.0	0.0	0.0
	15–0	6	0.0	0.0	0.0	0.0	20	*80*	0.0	0.0	0.0	0.0	0.0	0.0
1887	0–5	7	0.0	0.0	0.0	0.0	0.0	0.0	*100*	0.0	0.0	0.0	0.0	0.0
	5–15	8	0.0	0.0	0.0	0.0	0.0	0.0	25	*50*	25	0.0	0.0	0.0
	5–30	9	0.0	0.0	0.0	0.0	0.0	0.0	0.0	0.0	*100*	0.0	0.0	0.0
1808	0–5	10	0.0	0.0	0.0	0.0	0.0	0.0	12	0.0	0.0	*88*	0.0	0.0
	5–15	11	0.0	0.0	0.0	0.0	0.0	0.0	0.0	0.0	0.0	0.0	*100*	0.0
	15–30	12	0.0	0.0	0.0	0.0	0.0	0.0	0.0	0.0	25	0.0	0.0	*75*

[a] Seventy-six per cent of the original grouped cases were correctly classified. If only three factor scores were used, then 64% were correctly classified.

recent biomass in the 0–5 cm depth. Variation in factor two is responsible for the segregation of sites, with reasonable distinctions between 1808, 1872, 1885 blowdown sites and the virgin site. The virgin site is more closely associated with the recent blow down site (1985) at all depths. Factor two is most heavily influenced by m/z 76 (Fig. 4b), which is not a common product of recent biopolymer pyrolysis. One possibility is hydroxyacetic acid. Another important ion is m/z 46, which could be formic acid.

The carbohydrate-derived primary pyrolysis products occupy the same factor space as the 0–5 cm samples (Fig. 4b). The separation of the carbohydrates from the lignin-derived peaks is not as pronounced as would be expected based on the hypothesis that carbohydrates decompose more rapidly by microbial processes and that lignin and its alteration products are the predominant starting materials of the humic fraction. To the right of the lignin cluster in the loading plot are the series of mass variables, m/z 96, 95, 82, 69, 70 and 68. These are furan structures probably derived from altered carbohydrates that have persisted in the soil by cross-linking with the humic materials. Phenols are also in this region of the loading plot, which are most likely derived from lignin. Phenol, m/z 94, is to the right and cresol, 108, methyl cresol, 122, and catechol, 110 are

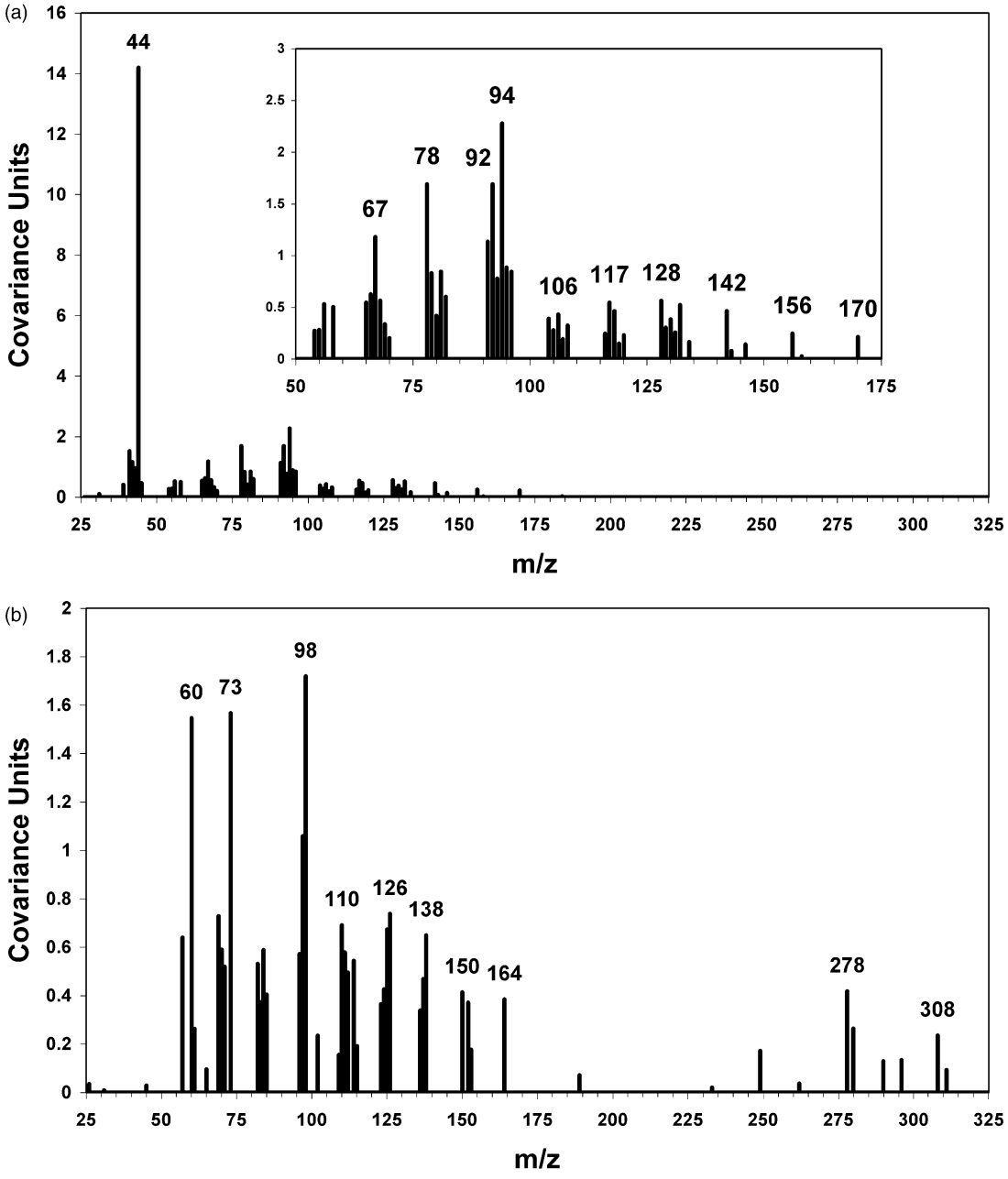

Fig. 5. Component spectra two (a) and three (b), based on pure masses m/z 78 and 73, respectively.

positioned to the left suggesting gradual changes in lignin composition with soil matter maturation. However, phenolics can also be formed from carbohydrates, especially when furans are dominant (Evans and Milne, 1987).

The extreme points in the loading plot (Fig. 4b) are used as targets to define new vectors, the component axes, that are calculated from the original factor analysis using the loading coefficients of the target mass. This facilitates chemical interpretation of the resulting components and allows scores for these components for each sample to be calculated. The self-modeling technique of Windig et al. (1987) was used for this and four components were calculated in this data set. The term "self-modeling" is used because the determination of components is done by the application of rules to the data. To determine the purity of the target masses (i.e. a mass which only has one source), the matrix of loadings is searched to find the longest vector lengths in the multidimensional loading matrix. This is confirmed visually by inspecting the graphs, such as Fig. 4b. This approach has advantages when working with data sets for which model compounds are not available and avoids problems associated with applying conceptions of what the samples should contain, such as picking a carbohydrate peak and a lignin peak, etc. There is little

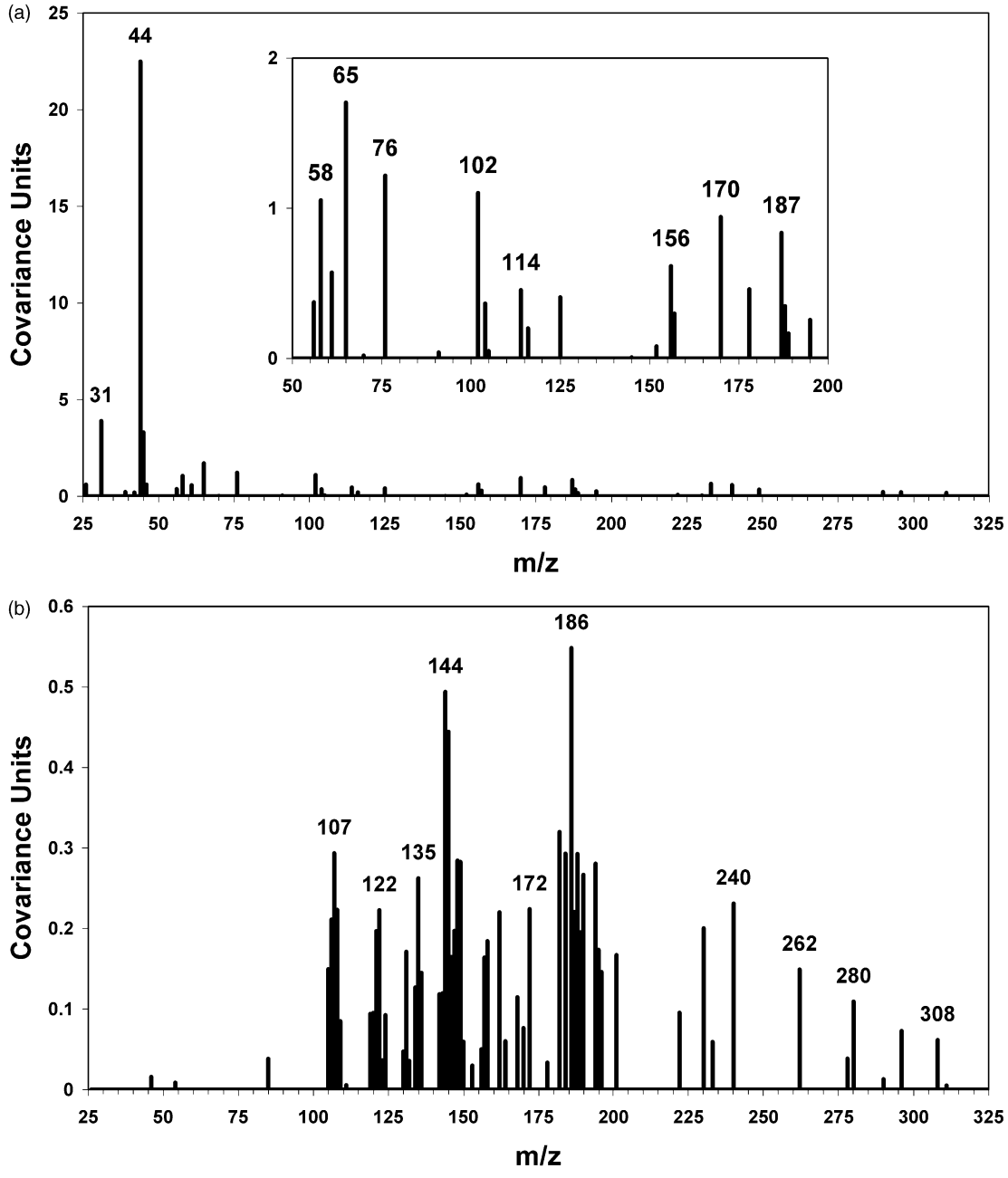

Fig. 6. Component spectra one (a) and four (b), based on pure masses m/z 76 and 186, respectively.

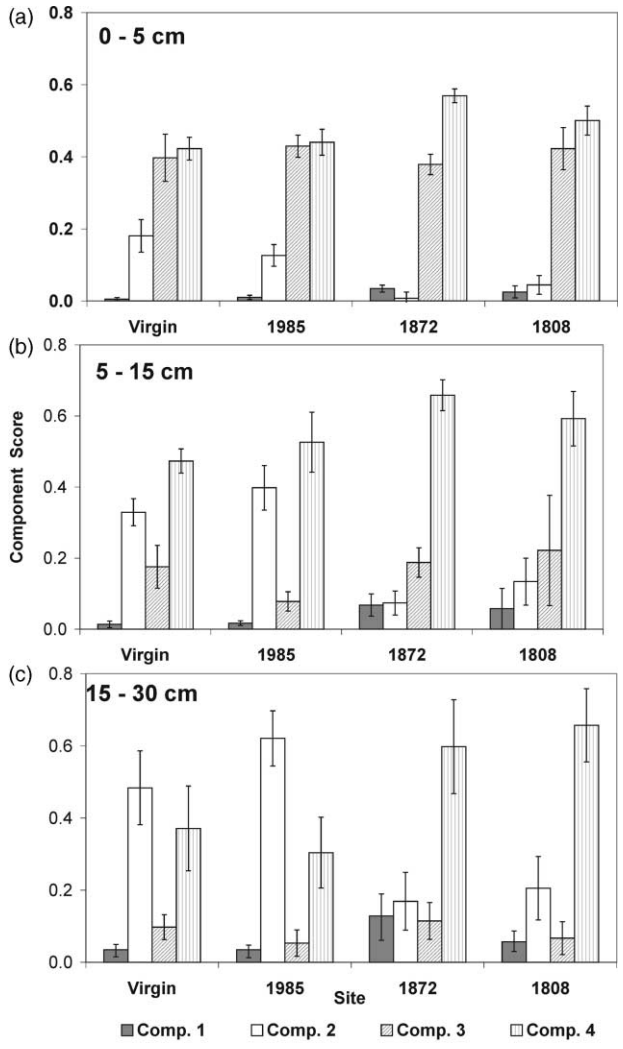

Fig. 7. Average component scores for the 12 groups of samples (four sites×three depth increments). Error bars show the 95% confidence intervals. Replication included both analytical and sampling variances.

doubt that the selection of four components in this case is an oversimplification of soil organic matter composition. However, considering the heterogeneity of soil samples and the complexity of the product spectrum, further analysis should be done before extending the method to a higher number of components. Details and examples of the self-modeling procedure can be found in the references (Windig et al., 1987; Agblevor et al., 1994).

The four "pure masses" chosen to calculate the component spectra for all of the samples in the data set were m/z 76, 78, 73, and 186. M/z 186 does not appear to be an extreme in Fig. 4b, but it has a high coefficient for factor three. The component spectra are calculated by first determining the length of each and every mass vector when projected on the pure mass vector. For example, in Fig. 4b, the pure mass 73 vector lies from the origin to the point labeled as 73. Other masses such as 60 and 114 will have shorter lengths when projected

Table 2
Pearson correlation coefficients (r) and significance level for $n=90$

		F001	F002	F003	F004
F001	r	1.000			
	Sig. (two-tailed)				
F002	r	−0.105	1.000		
	Sig. (two-tailed)	0.324			
F003	r	−0.269*	*−0.674***	1.000	
	Sig. (two-tailed)	0.010	*0.000*		
F004	r	0.139	−.0664**	−0.048	1.000
	Sig. (two-tailed)	0.193	*0.000*	0.656	

* Correlation is significant at the 0.05 level (two-tailed).
** Correlation is significant at the 0.01 level (two-tailed).

onto that vector. This new transformed loading matrix is essentially correlation coefficients ranging from −1 to 1. Each coefficient is then scaled to the standard deviation so that high relative intensity masses will appear as they do in the original data thus assisting visual interpretation. This is why the y-axis in Figs. 5 and 6 are labeled in covariance units.

Components two and three, based on m/z 78 and 73, are easily interpretable and give the index that was the goal of this work: to rapidly distinguish between recent (component three) and humic organic matter (component two) in soils. These two component spectra, which are mathematically derived profiles of mass variables, are shown in Fig 5. The largest mass peak in component spectrum two is m/z 44, assumed to be CO_2. Given that the other products in the spectrum are predominantly aromatics, the source of the CO_2 could be aromatic carboxylic acids, which we assume to be primarily derived from lignin precursors. Broadbent (1954) observed the carboxyl content of oat straw lignin increase from 80 to 140-meq/100 g over a year of incubation, suggesting that decomposition of lignin can result in increases in aromatic carboxylic acids.

The expanded upper mass range of component spectrum two is similar to the 15–30 cm spectrum shown in Fig. 3b, with a predominance of monoaromatics (benzene, 78; toluene, 92; and xylene, 106), phenolics (phenol, 94; cresol, 108); and polyaromatics (naphthalene, 128; and methylnaphthalenes, 142, 156, 170). The major nitrogen-containing compounds are pyrole, 67, pyridine, 79, aniline, 93, and indole, 117. Component two, therefore, appears to represent humified organic matter in these soils.

In contrast, the spectrum of component three shows peaks attributable to recent biomass, such as carbohydrate-derived peaks (m/z 60, 73, 98, 110, and 126) and lignin-derived peaks (m/z 110, 124, 138, 150, 152 and 164). The major peaks in the 0–5 cm soil samples (Fig. 2) at m/z 82 and 96 are not predominant in component spectrum three because they are common to both biopolymer and humic fractions. Two prominent

peaks in the higher mass range (e.g. m/z 278 and 308) are not characteristic of primary biopolymer products. The identification of these products is still to be determined.

Fig. 6 shows the other two component spectra, which are not easily identified. Component spectrum one (Fig. 6a) had m/z 76 as the pure mass and m/z 44 is predominant in this spectrum (as it was in component spectrum two). A possible structure for m/z 76 is hydroxyacetic acid, which could explain the fragment ion at m/z 31 (CH_3O) and the correlation with CO_2. The significance of the product distribution in component one is uncertain. M/z 65, an atypical fragment ion, also had characteristics of a pure mass when a fifth factor was considered. Therefore, component one may be more easily interpreted if resolved into two components. However, this was not done because of the uncertainty of this pure mass. Noise peaks can have many of the same characteristics of pure masses.

Fig. 6b (component spectrum four) shows another suite of products that are not attributable to known starting biomass structures. Phenols could be responsible for m/z 107, 108, 122 and 136. The pure mass and largest peak is m/z 186, which could be $C_{11}H_{22}O_2$, a possible saturated fatty acid that could be part of a series of organic acids at m/z 144, 158, 172, and 186 ($C=8$ to 11). The higher molecular weight peaks are not attributable to known products or starting materials. One possibility is that this component includes the nonpolar materials, such as fats, waxes, and resins, which are known to be constituents of SOM (Schulten, 1996). It is also possible that component spectrum one and four are the result of microbial changes in humification. They may also be due to the change in vegetation that the sites under went after the wind event disrupted the virgin beech hemlock forest system.

The relative amounts of the four components in the sample set are shown in Fig. 7 for the virgin, the 1985, the 1872 and 1808 sites as a function of depth increment. Error bars show the 95% confidence intervals, which reflect both sampling and analytical uncertainties. Component one (Fig. 6a) is a minor amount in all cases and has a limited presence in the virgin and 1985 sites. Higher amounts are observed in the 1872 and 1808 sites. The relative amount of component one may increase with depth but variability was great ($r=0.46$).

Component two (Fig. 5a), the aromatic humic products, increased with depth ($r=0.89$) and is significantly higher in the virgin and 1985 sites versus the 1872 and 1808 sites. The stability of the material giving rise to this component would be expected to be very high so its systematic change may reflect the impact of changing vegetation over time.

Component three (Fig. 5b), the recent biomass products, is not significantly different between sites at any depth increment. It significantly decreases with depth ($r=-0.87$) with a reduction of 50% in the 5–15 cm depth and another 50% reduction in the 15–30 cm

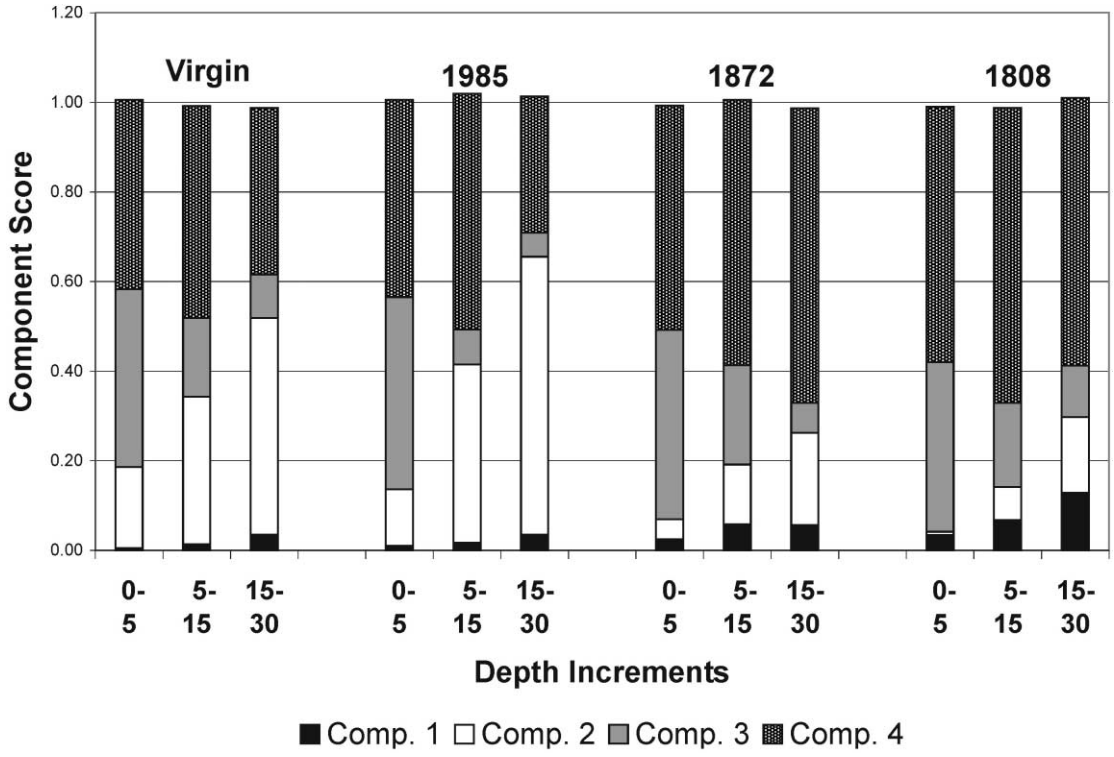

Fig. 8. The average component scores for all runs at each depth and site.

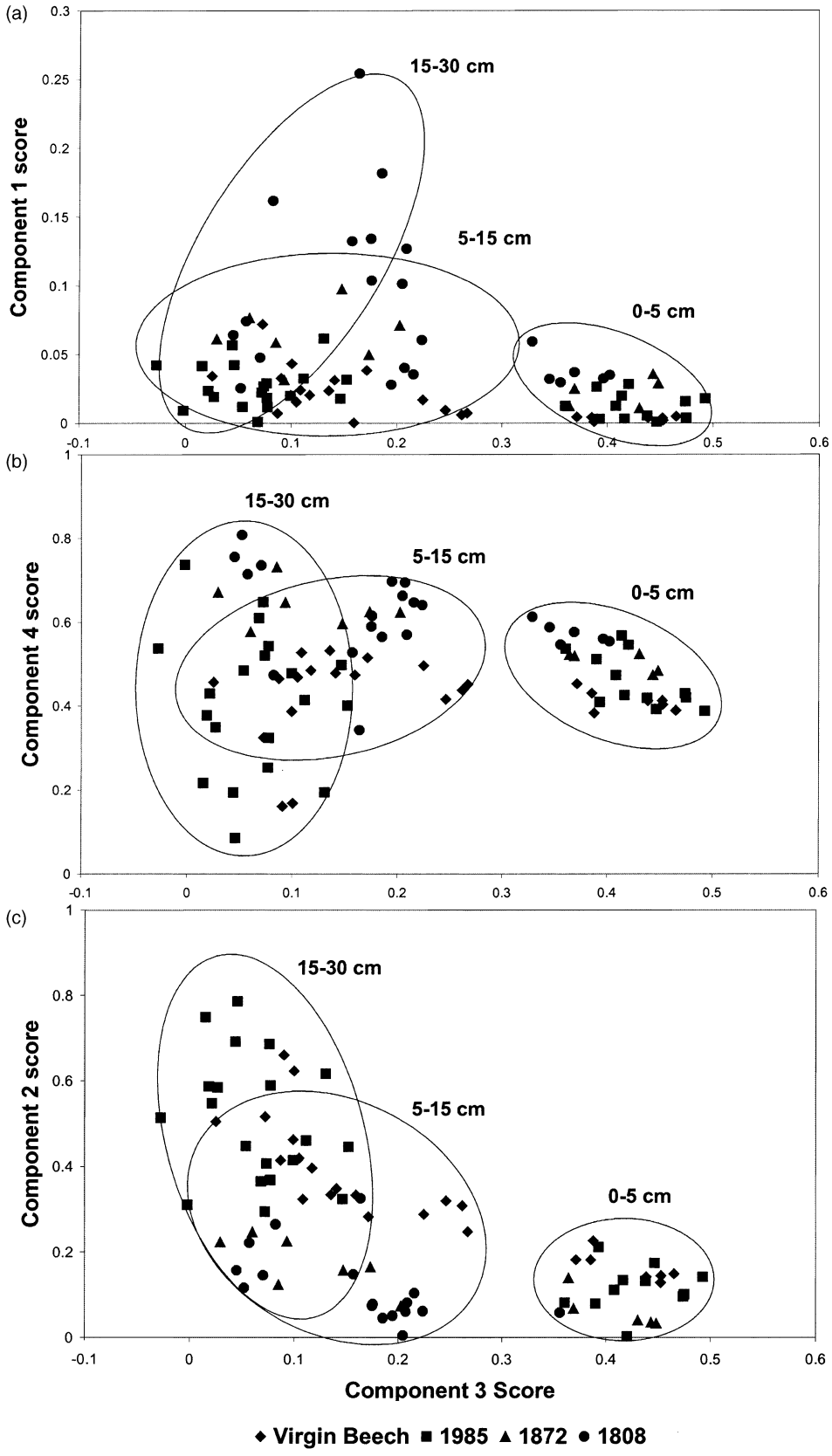

Fig. 9. Scatter plots showing comparisons between components (a) one and three, (b) four and three, and (c) two and three for all depths at all sites.

depth, which is consistent with the characterization of this component as recent organic matter.

Component four (Fig. 6b) does not vary systematically with depth ($r = -0.09$), but does vary with site; higher values are observed for the 1872 and 1808 sites at all depths. Unlike the other unknown, component one, which was a minor fraction of the total, component four accounts for a significant fraction of the soil organic matter.

Fig. 8 shows the average for all runs at each depth and site. This presentation makes the trends more visible. Table 2 shows the correlation coefficients and level of significances for the four components across the whole data set. Components two and three and two and four are negatively correlated, but three is not correlated with four.

The scatter plots in Fig. 9 show the bivariate comparisons relative to component three, the recent biomass fraction. Sites are shown by symbols and sampling depth by ellipses. These plots show the same type of class separation as the factor score plot in Fig. 4a, but based on the resolved components rather than the original factors. The recent material (component three) completely separated the 0–5 cm depth interval, which is reasonable since the top layer is more influenced by recent soil organic matter than the other depths, either in the form of recent litter or roots. The plot of component three versus component two shows an inverse relationship ($r = -0.674$) and hence may be a possible indicator of recent versus humic materials in these soils. However, when only samples within the 0–5 cm depth profile are considered, there is no correlation between components three and two ($r = -0.10$). In the plot of component three versus four there is no correlation between component three and four ($r = -0.048$) although when the 0–5 cm class is considered alone there is a correlation ($r = -0.55$). The plot of component three versus component one is dominated by the 1808 site in the 15–30 cm depth profile.

4. Conclusion

The analysis of pyrolysis products of forest soil samples using py-MBMS and pattern recognition techniques showed an increase in pyrolysis products of more highly decomposed plant materials as a function of increasing sample depth. Recent biomass is characteristic of shallow samples and more aromatic species, representative of more degraded biomass, are found in the deeper samples. This technique could also distinguish among samples of different ecological sites. With continued development, this rapid analytical technique offers the opportunity to greatly increase our understanding of the role of SOM in carbon sequestration and carbon cycling, and to assess how forest management practices can enhance that role.

Acknowledgements

Special thanks to Harry Steele (USDA Forest Service) for extensive help with site selection and sampling and Michael Looker (NREL) for technical support of the MBMS. The authors also wish to thank Richard Birdsey (USDA Forest Service) for supporting the conventional combustion work and Susan Stout (USDA Forest Service) and Gene Peterson (National Renewable Energy Laboratory) for management support. This paper was presented at the USDA Forest Service Southern Global Change Program sponsored Advances in Terrestrial Ecosystem: Carbon Inventory, Measurements, and Monitoring Conference held 3–5 October 2000 in Raleigh, North Carolina.

References

Agblevor, F.A., Evans, R.J., Johnson, L.D., 1994. Molecular-beam mass spectrometric analysis of lignocellulosic materials. I. Herbaceous biomassa. J. Anal. Appl. Pyrol. 30, 125–144.

Beyer, L., Deslis, K., Vogt, B., 1998. Estimation of soil organic matter composition according to a simple thermoanalytical approach. Commun. Soil Sci. Plant Anal. 29 (9–10), 1277–1297.

Broadbent, F.E., 1954. Modification in chemical properties of straw during decomposition. Soil Sci. Soc. Am. Proc. 18, 165–169.

Evans, R.J., Milne, T.A., 1987. Molecular characterization of the pyrolysis of biomass. Energy and Fuels 1, 123–137.

Evans, R.J., Milne, T.A., Soltys, M.N., 1986. Direct mass-spectrometric studies of the pyrolysis of carbonaceous fuels. III. Primary pyrolysis of lignin. J. Anal. Appl. Pyrolysis 9, 207–236.

Evans, R.J., Milne, T.A., Soltys, M.N., Schulten, H.R., 1984. Mass spectrometric behavior of levoglucosan under different ionization conditions and implications for studies of cellulose pyrolysis. J. Anal. Appl. Pyrolysis 6, 273–283.

Gregorich, E.G., Monreal, C.M., Schnitzer, M., Schulten, H.R., 1996. Transformation of plant residues into soil organic matter: chemical characterization of plant tissue, isolated soil fractions, and whole soils. Soil Sci. 161 (10), 680–693.

Hempfling, R., Schulten, H.R., 1990. Direct chemical characterization of dissolved organic matter in water by pyrolysis-field ionization mass spectrometry. Int. J. Environ. Anal. Chem. 43, 55–62.

Hoover, C.M., Magrini, K.A., Evans, R.J., 2002. Soil carbon content and character in an old growth forest in northwestern Pennsylvania: a case study introducing molecular beam mass spectrometry (PY-MBMS). Environmental Pollution 116 (Supp. 1), S269–S278.

Leinweber, P., Schulten, H.R., Korschens, K., 1993. Seasonal variations of soil organic matter in a long-term agricultural experiment. Plant Soil 160, 225–235.

Leinweber, P., Jordan, E., Schulten, H.R., 1996. Molecular characterization of soil organic matter in Pleistocene moraines from the Bolivian Andes. Geoderma 72 (1–2), 133–148.

Milne, T.A., Soltys, M.N., 1983. Direct mass-spectrometric studies of the pyrolysis of carbonaceous fuels. II. Qualitative observations of primary and secondary processes in biomass. J. Anal. Appl. Pyrolysis 5, 93–131.

Ogner, G., Schnitzer, M., 1971. Chemistry of fulvic acid, a soil humic fraction, and its relation to lignin. Can. J. Chem. 49 (7), 1053–1063.

Reeves, J.B., McCarty, G.W., Mesinger, J.J., 1999. Near infrared spectroscopy for the analysis of agricultural soils. J. Near Infrared Spectrosc. 7 (3), 179–193.

Rosenberg, N.J., Izaurralde, R.C., Malone, E.L. (Eds.), 1998. Carbon sequestration in soils: science, monitoring, and beyond. Proceedings of the St. Michaels Workshop. Batelle Memorial Press, Columbus, OH.

Salgo, A., Nagy, J., Tarnoy, J., Marth, P., Palmai, O., Szabo-Kele, G., 1998. Characterization of soils by the near infrared technique. J. Near Infrared, Spectroscopy 6 (1–4), 199–203.

Scharpenseel, H.W., 1975. Relative age and age sequence of fractions of soil organic matter. Newsl. Appl. Nucl. Methods Biol. Agric 5, 10–17.

Schepers, J.S., Francis, D.D., Thompson, M.T., 1989. Simultaneous determination of total carbon, total nitrogen, and nitrogen-15 on soil and plant material. Commun. Soil Sci. Plant Anal. 20 (9–10), 949–959.

Schulten, H.R., 1996. Direct pyrolysis-mass spectrometry of soils: a novel tool in agriculture, ecology, forestry, and soil science. In: Boutton, T.W., Yamasaki, S.-H. (Eds.), Mass Spectrometry of Soils. Marcel Dekker, New York, NY, pp. 373–436.

Schulten, H.R., Leinweber, P., 359-. Advances in analytical pyrolysis of soil organic matter. J. Anal. Appl. Pyrolysis 49 (1–2).

SPSS Inc, 1999. SPSS Base 10.0 Applications Guide. SPSS Inc, Chicago, IL. Available at: http://www.spss.com.

Stuczynski, T.I., McCarty, G.W., Reeves, J.B., Wright, R.J., 1997. Use of pyrolysis GC/MS for assessing changes in soil organic matter quality. Soil SCI. 162 (2), 97–105.

Tao, Z.Y., Liu, S.F., Zhai, J.J., Sheng, F.L., 1997. Studies of thermal transformations of humic and fulvic acids in soils. Part 1. Infrared spectroscopy and temperature-programmed pyrolysis mass spectrometry. Chem. Ecol. 13 (4), 237–248.

Tresar-Cepeda, M.C., Ceccanti, B., Leiros, M.C., Calcinai, M., Gil-Sotres, F., 1994. Characterization of organic matter in lignite mine soils at various ages by pyrolysis/gas chromatography. In: Senesi, N., Miano, T.M., (Eds.), Humic Subst. Global Environ. Implic. Hum. Health, Proc. Int. Meet. Int. Humic Subst. Soc., 6th, Amsterdam, pp. 707–712.

Tuskan, G., West, D., Bradshaw, H.D., Neale, D., Sewell, M., Wheeler, N., Megraw, B., Jech, K., Wiselogel, A., Evans, R., Elam, C., Davis, M., Dinus, R., 1999. Two high-throughput techniques for determining wood properties as part of a molecular genetics analysis of hybrid poplar and loblolly pine. Appl. Biochem. Biotechnol. (Twentieth Symposium on Biotechnology for Fuels and Chemicals, 1998) 77–79, 55–65.

Wilcken, H, Sorge, C., Schulten, H.R., 1997. Molecular composition and chemometric differentiation and classification of soil organic matter in Podzol B-horizons. Geoderma 76 (3–4), 193–219.

Windig, W., McClennen, W.H., Muezelaar, H.L.C., 1987. Chemometrics and Intelligent Lab. Systems 1, 151–165.